Am J Otolaryngol 40 (2019) 191–196

Contents lists available at ScienceDirect

Am J Otolaryngol

journal homepage: www.elsevier.com/locate/amjoto

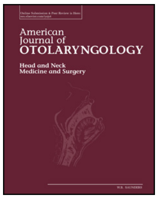

Identification of key genes and pathways in chronic rhinosinusitis with nasal polyps using bioinformatics analysis

Yao Yao, Shaobing Xie, Fengjun Wang*

[a] *Department of Otolaryngology Head and Neck Surgery, Xiangya Hospital of Central South University, Changsha, Hunan, China*
[b] *Province Key Laboratory of Otolaryngology Critical Diseases, Changsha, Hunan, China*

ARTICLE INFO

Keywords:
Chronic rhinosinusitis
Nasal polyps
Microarray
Bioinformatics analysis
Hub gene
Pathway

ABSTRACT

Purpose: Chronic rhinosinusitis with nasal polyps (CRSwNP) is a prevalent inflammatory disease of yet unknown etiology. The purpose of this study was to uncover key genes and pathways related to the pathogenesis of CRSwNP via bioinformatics approaches.
Materials and methods: The gene expression profile of GSE36830 extracted from Gene Expression Omnibus database was used to screen differentially expressed genes (DEGs) between nasal polyp samples and control samples. Furthermore, functional and pathway enrichment analysis was performed using the clusterProfiler package in R language. In addition, protein-protein interaction (PPI) network was constructed by STRING database and functional modules were detected using Molecular Complex Detection algorithm.
Results: A total of 538 DEGs (326 up-regulated and 212 down-regulated) were identified. The most significantly enriched pathways for up-regulated and down-regulated genes were hematopoietic cell lineage and salivary secretion, respectively. Moreover, twenty hub genes with high connectivity degrees were selected from the PPI network, such as TYRO protein tyrosine kinase binding protein (TYROBP), G protein subunit gamma 2 (GNG2), CCR7, and CCR3. Besides, six important modules were obtained, which were highly associated with chemokine signaling pathway, Th1 and Th2 cell differentiation, complement and coagulation cascades, cell cycle, systemic lupus erythematosus, and *Staphylococcus aureus* infection.
Conclusions: The results of this study may provide new insights into potential molecular mechanisms of CRSwNP. Nevertheless, further experiments are needed to confirm these findings.

1. Introduction

Chronic rhinosinusitis with nasal polyps (CRSwNP) is defined as a complex and persistent inflammatory condition characterized by the presence of edematous masses in the nasal and paranasal cavities [1,2]. CRSwNP is associated with significant morbidity and seriously compromises patients' quality of life (QOL) and productivity [3]. In general, CRSwNP shows a Th2-biased inflammation with excessive eosinophil infiltration and high levels of IgE, particularly in Western countries [4]. Despite advances in medical therapy and surgical intervention, management of patients with CRSwNP is still unsatisfactory, and the recurrence is frequent [5]. Thus, more insights into the pathogenesis of CRSwNP are needed to develop effective therapeutic strategies.

In recent years, high-throughput microarray technologies have been widely used to capture the global gene expression patterns in diverse human diseases, including CRSwNP [6–8]. As a result, a series of gene expression datasets have been generated and stored in the public repositories, such as Gene Expression Omnibus (GEO) and ArrayExpress [9,10]. Nevertheless, large numbers of microarray data have not been fully utilized. These data can be reanalyzed with the latest bioinformatic algorithms, unveiling new molecular mechanisms [11,12]. Therefore, in the present study, we downloaded the publicly available gene expression data related to CRSwNP and applied bioinformatic tools to identify the different gene signatures between polyp samples and control samples. Moreover, the possible biological functions and signaling pathways of differentially expressed genes (DEGs) were enriched. In addition, protein-protein interaction (PPI) network was constructed to find the critical genes and modules in CRSwNP. Hopefully, our findings may contribute to a better understanding of the pathomechanism of CRSwNP and provide potential pharmacological targets for further studies.

---

* Corresponding author at: Department of Otolaryngology Head and Neck Surgery, Xiangya Hospital of Central South University, 87 Xiangya Road, Changsha 410000, Hunan, China.
E-mail address: xyyyentwfj@hotmail.com (F. Wang).

https://doi.org/10.1016/j.amjoto.2018.12.002
Received 8 November 2018

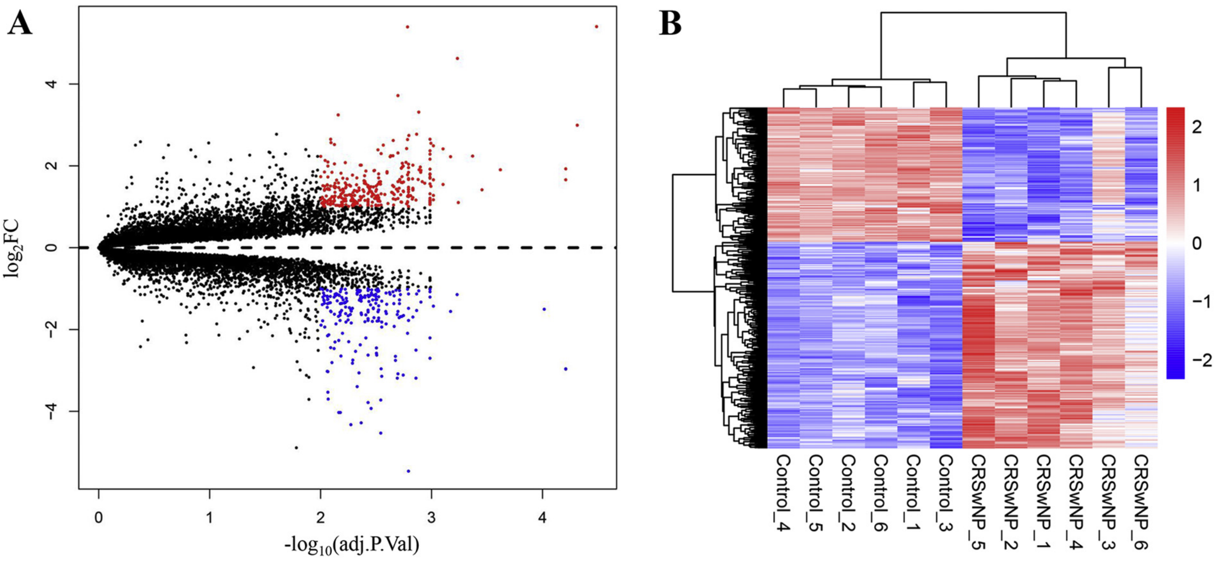

Fig. 1. Identification of DEGs in CRSwNP. (A) Volcano plot of DEGs between polyp samples and control samples. Red and blue points represent up- and down-regulated DEGs, respectively. Black points indicate genes with no significant difference. (B) Hierarchical clustering heatmap of polyp samples and control samples based on identified DEGs. Each row represents a single gene and each column represents a sample. Blue, white, and red colors indicate low, intermediate, and high relative expression, respectively. (For interpretation of the references to colour in this figure legend, the reader is referred to the web version of this article.)

2. Materials and methods

2.1. Acquisition of gene expression profiling data

The microarray data of GSE36830 deposited by Kato et al. [13] was retrieved from the GEO database (http://www.ncbi.nlm.nih.gov/geo/). The gene expression profile was generated with GPL570 Affymetrix Human Genome U133 Plus 2.0 Array (Affymetrix, Santa Clara, CA, USA). A total of 12 specimens, including six nasal polyp samples from patients with CRSwNP and six uncinate tissue samples from control subjects, were selected for further analysis. Briefly, each sample was obtained from a different patient. Patients with CRSwNP were diagnosed according to the American Academy of Otolaryngology-Head and Neck Surgery Chronic Rhinosinusitis Task Force guidelines [14]. Control patients who underwent endoscopic skull-base tumor excisions had no history of upper airway inflammatory diseases [13].

2.2. Raw data preprocessing and screening of DEGs

First, background correction and standardization of the raw data were conducted by Robust Multi-array Average (RMA) algorithm using the affy package in R language [15]. Subsequently, probe IDs were mapped to official gene symbols according to annotation information. If multiple probes corresponded to the same gene symbol, the expression values of those probes were averaged. In the end, a total of 20,486 gene expression values were achieved.

Next, gene expression differences between polyp tissues and control tissues were determined using the limma package with the Empirical Bayes method [16]. The Benjamini-Hochberg false discovery rate (FDR) was used to correct for P value. In this study, adjusted P value < 0.01 and $|\log_2(\text{fold change})|$ ($|\log_2\text{FC}|$) > 1.0 were set as the cut-off criteria to screen for DEGs. Furthermore, the volcano map was plotted according to the adjusted P value and $\log_2$FC. In addition, hierarchical clustering analysis of polyp samples and control samples based on DEGs was performed and visualized using the pheatmap package in R language.

2.3. Functional and pathway enrichment analysis

To explore biological functions and involved pathways of significant up- and down-regulated DEGs, Gene Ontology Biological Process (GO-BP) and Kyoto Encyclopedia of Genes and Genomes (KEGG) enrichment analyses were performed using the clusterProfiler package in R language [17]. The thresholds for these analyses were set as adjusted P value < 0.05 and gene count ≥ 2.

2.4. PPI network construction and module analysis

Search Tool for the Retrieval of Interacting Genes (STRING; http://www.string-db.org/) is a powerful online tool and biological database that provides a variety of known and predicted interaction information for researchers [18]. Identified DEGs were scanned by the STRING database, and then PPI network was constructed. The combined score ≥ 0.700 was set as the cut-off criterion, which indicated that only interactions with high level of confidence were considered as valid links for the PPI network. Furthermore, PPI network was embodied using the Cytoscape software (http://www.cytoscape.org/). In the network, each node represents a gene and the edge represents a connection between the nodes. The degree of node represents the number of interaction partners. Nodes with high degrees are assumed to represent the hub genes possessing important biological functions.

The Molecular Complex Detection (MCODE), a plug-in in Cytoscape software, was subsequently employed to extract significant modules from the PPI network based on graph-theoretic clustering algorithm [19]. We used this tool with the following parameter setting: degree cutoff = 2, node score cutoff = 0.2, k-core = 3, max. depth = 100. In addition, the KEGG pathway enrichment analysis of genes in each module was performed by the clusterProfiler package in R language.

3. Results

3.1. Identification of DEGs in CRSwNP

After preprocessing of the raw dataset, a total of 538 DEGs (326 up-regulated and 212 down-regulated) were identified in polyp tissues when compared to control tissues (Fig. 1A). Hierarchical clustering analysis based on these DEGs revealed clear separation of patients with CRSwNP from control subjects (Fig. 1B). The top 10 up- and down-regulated DEGs ranked by $\log_2$FC in CRSwNP are listed in Table 1. Notably, many of the top 10 up-regulated genes in CRSwNP have been

Table 1
Top 10 up- and down-regulated DEGs in CRSwNP.

Category	Gene symbol	Description	$\log_2$FC	Adjusted *P* value
Up-regulated	CCL13	C-C motif chemokine ligand 13	5.402	3.25E−05
	CLC	Charcot-Leyden crystal galectin	5.397	1.65E−03
	CCL18	C-C motif chemokine ligand 18	4.629	5.84E−04
	SCG2	Secretogranin II	3.715	2.00E−03
	CCL8	C-C motif chemokine ligand 8	3.311	1.30E−03
	RNASE2	Ribonuclease, RNase A family, 2	3.247	6.95E−03
	F13A1	Coagulation factor XIII, A1 polypeptide	2.991	4.87E−05
	SIGLEC1	Sialic acid binding Ig-like lectin 1	2.777	1.36E−03
	EMR1	EGF-like module containing, mucin-like, hormone receptor-like 1	2.744	1.60E−03
	CD300LF	CD300 molecule-like family member f	2.653	1.04E−03
Down-regulated	PRB3	Proline-rich protein BstNI subfamily 3	−5.462	1.62E−03
	PRB4	Proline-rich protein *Bst*NI subfamily 4	−4.531	2.87E−03
	BPIFB2	BPI fold containing family B, member 2	−4.327	5.34E−03
	LPO	Lactoperoxidase	−4.279	4.32E−03
	PRB1	Proline-rich protein BstNI subfamily 1	−4.027	6.88E−03
	HTN3	Histatin 3	−4.025	6.64E−03
	MUC19	Mucin 19, oligomeric	−3.932	3.52E−03
	TFF1	Trefoil factor 1	−3.783	3.73E−03
	HP	Haptoglobin	−3.723	2.87E−03
	GP2	Glycoprotein 2 (zymogen granule membrane)	−3.700	8.54E−03

FC = fold change.

suggested to play crucial roles in induction of type 2 inflammation and eosinophil migration, such as CCL13, CCL18, CCL8, Charcot-Leyden crystal galectin (CLC), and EGF-like module containing, mucin-like, hormone receptor-like 1 (EMR1) [20–22]. On the other hand, most of the top 10 genes with the greatest degree of downregulation are related to antimicrobial defense responses, such as proline-rich protein *Bst*NI subfamily 3 (PRB3), BPI fold containing family B, member 2 (BPIFB2), lactoperoxidase (LPO), histatin 3 (HTN3), and haptoglobin (HP) [23–27].

3.2. GO-BP and KEGG enrichment analyses of DEGs

To gain further insights into pathological mechanisms of CRSwNP, up- and down-regulated DEGs were subjected to functional enrichment and pathway analysis, respectively. The results are presented in Tables 2 and 3. GO-BP enrichment analysis demonstrated that up-regulated DEGs were mainly concentrated in leukocyte cell-cell adhesion, activation, and differentiation. The down-regulated DEGs were significantly enriched in response to xenobiotic stimulus and secretion by tissue. As for KEGG enrichment analysis, the top 5 enriched pathways for up-regulated DEGs included hematopoietic cell lineage, *Staphylococcus aureus* infection, cell adhesion molecules, chemokine signaling pathway, and primary immunodeficiency. Moreover, the significantly enriched pathways for down-regulated DEGs contained salivary secretion and choline metabolism in cancer.

Table 3
Top KEGG pathways in the enrichment analysis of up- and down-regulated DEGs associated with CRSwNP.

Category	Pathway	Gene count	Adjusted *P* value
Up-regulated	Hematopoietic cell lineage	17	3.71E−09
	Staphylococcus aureus infection	13	1.20E−08
	Cell adhesion molecules (CAMs)	18	9.93E−08
	Chemokine signaling pathway	20	1.70E−07
	Primary immunodeficiency	9	2.46E−06
	Osteoclast differentiation	14	1.94E−05
	Cytokine-cytokine receptor interaction	21	3.58E−05
	Leishmaniasis	10	9.29E−05
	Leukocyte transendothelial migration	12	1.06E−04
	Phagosome	13	4.58E−04
	Asthma	6	7.79E−04
	Complement and coagulation cascades	9	7.79E−04
Down-regulated	Salivary secretion	8	1.58E−03
	Choline metabolism in cancer	7	1.28E−02

3.3. Analysis of the PPI network

To better understand functional interrelationships among DEGs, we utilized STRING database to construct the PPI network. This PPI

Table 2
Top GO-BP terms in the enrichment analysis of up- and down-regulated DEGs associated with CRSwNP.

Category	Term	Gene count	Adjusted *P* value
Up-regulated	Leukocyte cell-cell adhesion	42	2.85E−19
	T cell activation	43	9.67E−17
	Positive regulation of cell activation	38	9.67E−17
	Regulation of T cell activation	36	9.67E−17
	Regulation of leukocyte cell-cell adhesion	37	9.67E−17
	Regulation of lymphocyte activation	41	5.83E−16
	Regulation of cell-cell adhesion	39	2.01E−15
	Positive regulation of leukocyte activation	35	5.11E−15
	Positive regulation of leukocyte cell-cell adhesion	29	5.11E−15
	Positive regulation of T cell activation	28	1.15E−14
	Leukocyte differentiation	39	7.60E−14
	Positive regulation of cell-cell adhesion	29	1.57E−13
Down-regulated	Response to xenobiotic stimulus	8	3.70E−02
	Secretion by tissue	5	3.70E−02

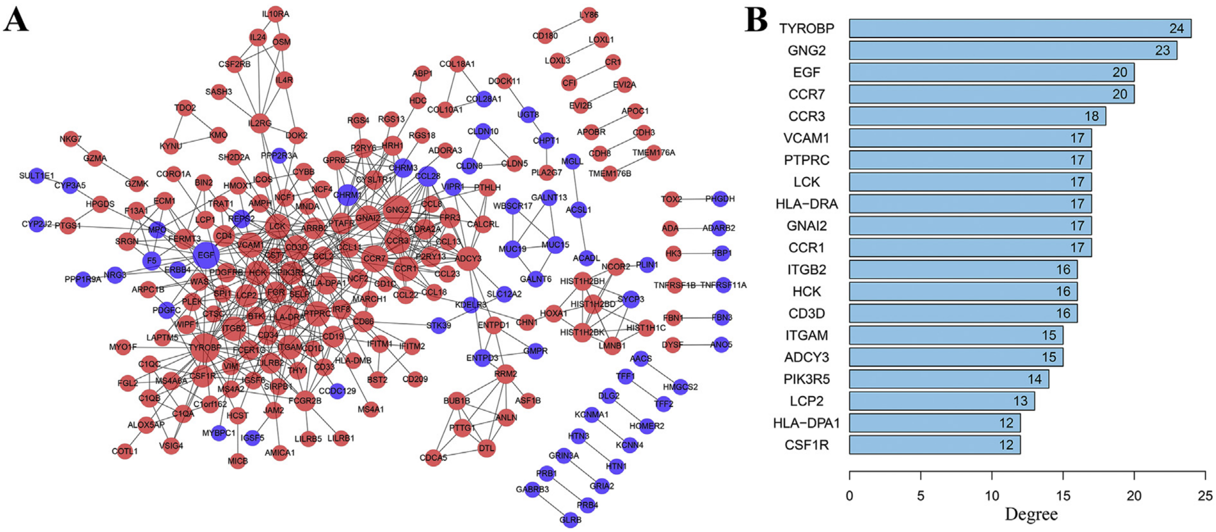

Fig. 2. Analysis of the PPI network. (A) PPI network of DEGs constructed by STRING database and Cytoscape software. Red and blue circles represent up- and down-regulated genes, respectively. The size of the circles is proportional to node degrees. (B) Hub genes identified from the PPI network. The y-axis represents the name of genes, and the x-axis represents the number of adjacent genes. (For interpretation of the references to colour in this figure legend, the reader is referred to the web version of this article.)

network was composed by 229 nodes and 513 edges (Fig. 2A). Furthermore, we analyzed the topological structure of the PPI network and achieved the degree of each node. Herein, we selected the top 20 nodes with high degrees as hub genes (Fig. 2B). Of these hub genes, TYRO protein tyrosine kinase binding protein (TYROBP) and G protein subunit gamma 2 (GNG2) showed the higher degree values, which were 24 and 23, respectively.

3.4. Module screening from the PPI network

Next, we used MCODE algorithm to detect densely connected regions from our PPI network. Also, KEGG enrichment analysis was performed to explore most significantly enriched pathway for each module. As a result, a total of 6 modules were obtained (Fig. 3), representing distinct biological pathways. Module 1 (MCODE score = 10) consisted of 10 DEGs implicated in chemokine signaling pathway (adjusted *P* value = 4.68E − 08). Module 2 (MCODE score = 6.769) contained 14 DEGs related to Th1 and Th2 cell differentiation (adjusted *P* value = 7.89E − 06). Module 3 (MCODE score = 5) comprised 5 DEGs associated with complement and coagulation cascades (adjusted *P* value = 6.58E − 04). Module 4 (MCODE score = 5) included 5 DEGs enriched in cell cycle (adjusted *P* value = 6.49E − 03). Module 5 (MCODE score = 5) included 5 DEGs involved in systemic lupus erythematosus (adjusted *P* value = 2.69E − 04). Module 6 (MCODE score = 3.867) contained 16 DEGs enriched in *Staphylococcus aureus* infection (adjusted *P* value = 4.89E − 08).

4. Discussion

CRSwNP represents a common chronic inflammatory disorder of the

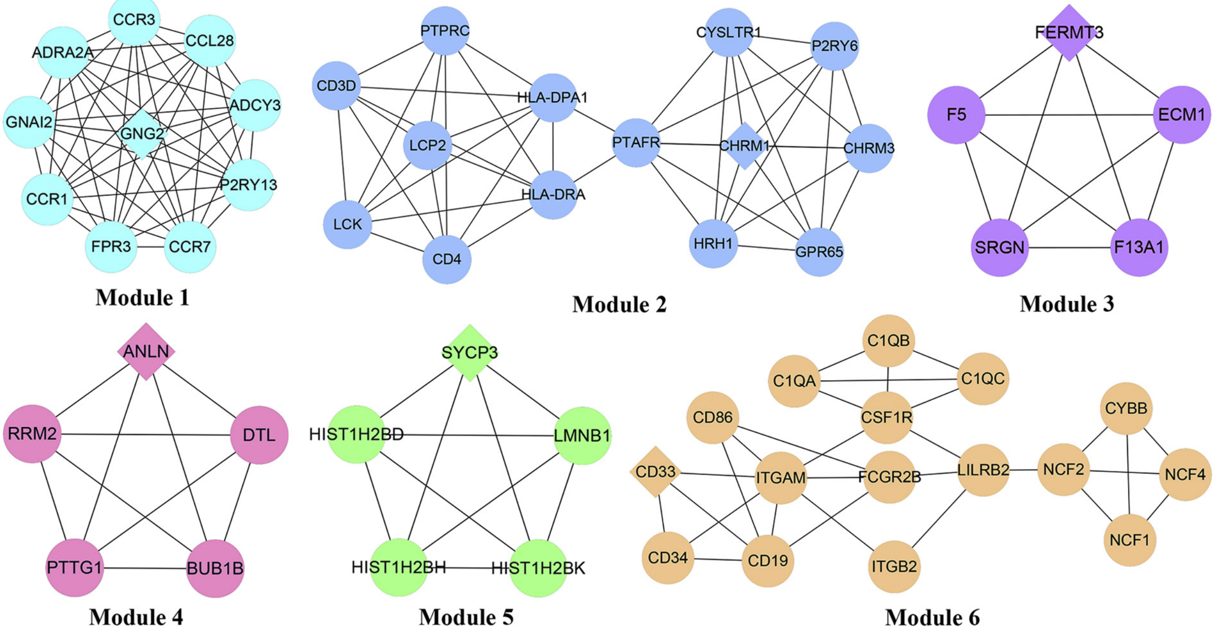

Fig. 3. Six modules extracted from the PPI network. Nodes stand for the genes and edges stand for the interactions of genes. Diamonds represent seed nodes.

upper airways and is difficult to treat [1,2]. Given the complicated and multifactorial nature of CRSwNP [28], there is an urgent need to explore the underlying molecular mechanisms of this disease. Bioinformatics, a new discipline that combines biological sciences and computational and statistical techniques, has remarkable ability to uncover novel biological insights. Hence, in this paper, we extracted the data from GSE36830 and systematically analyzed the differential gene expression between polyp samples and control samples using multiple bioinformatic approaches, including functional and pathway enrichment analysis, PPI network construction, and module screening from the PPI network.

We identified 326 up-regulated and 212 down-regulated genes in patients with CRSwNP in comparison with controls. Based on KEGG enrichment analysis, the most significantly enriched pathway for up-regulated DEGs was hematopoietic cell lineage. This is consistent with the knowledge that various inflammatory cells participate in the occurrence and development of CRSwNP, such as eosinophils, basophils, group 2 innate lymphoid cells (ILC2s), dendritic cells (DCs), mast cells, macrophages, and lymphocytes [29]. On the other hand, the most markedly enriched pathway for down-regulated DEGs was salivary secretion. Several genes involved in salivary secretion were that encoding antimicrobial peptides (AMPs), such as PRB1, LPO, HTN1, and HTN3 [23,25,26]. Dysregulation of this pathway in CRSwNP might result in a primary defect in innate defense responses, thus increasing susceptibility to microbial colonization and contributing to ongoing inflammation in sinonasal mucosa.

Network-based analysis is a promising strategy to reflect complex interaction patterns among DEGs at system level. Therefore, PPI network was constructed for all the DEGs, and then topology properties of the PPI network were analyzed to detect hub genes. As a result, TYROBP was determined as one of the hub genes exhibiting the highest node degree. TYROBP, also known as DNAX-activating protein of 12 kDa (DAP12), encodes a transmembrane signaling adaptor protein that couples to numerous immunoregulatory receptors expressed on myeloid cells and natural killer (NK) cells [30,31]. Accumulating evidence has demonstrated that TYROBP has dual effects, either activating or inhibitory, on inflammatory and immune responses, depending on its microenvironment [32–34]. Although Lee et al. [35] have confirmed the upregulation of TYROBP in polyp tissues using semiquantitative real-time polymerase chain reaction (RT-PCR), there have been no reports concerning the precise role of TYROBP in the pathogenesis of CRSwNP. Hub genes with high connectivity degrees tend to have critical biological activities. Thus, we speculated that TYROBP could be a potential important biomarker for CRSwNP. Further studies of TYROBP may hold promise for the development of novel treatment strategies for CRSwNP.

Another hub gene, GNG2, encodes a G protein γ2 subunit involved in various biological functions, including cell proliferation, cell differentiation, platelet activation, as well as angiogenesis [36]. Leung et al. [37] have suggested that depletion of GNG2 alone in developing zebrafish embryos abolishes the ability of vascular endothelial growth factor (VEGF) to promote the angiogenic process. Since VEGF has been shown to play a pivotal role in edema formation in CRSwNP [38], blocking GNG2 may be an effective pharmacological method to suppress pathologic angiogenesis and polyp growth. However, further studies should be conducted to validate our findings.

As a large network can be decomposed into several small subnetworks for further functional analysis, we employed MCODE plug-in to detect highly connected areas from the PPI network. In the present study, a total of 6 modules were identified. Module 1 had the highest MCODE score, and was intensively associated with chemokine signaling pathway, due to the presence of GNG2, CCR1, CCR3, CCR7, CCL28, G protein subunit alpha i2 (GNAI2), and adenylate cyclase 3 (ADCY3). Remarkably, these seven DEGs were closely interacted in module 1, and most of them were regarded as hub genes in our PPI network. It has been well documented that chemokines, their receptors, and chemokine signal transduction are responsible for the maturation, recruitment, and activation of leukocytes at inflammation sites [39]. Consequently, analysis of this pathway could enhance our understanding of leukocyte trafficking mechanisms in CRSwNP.

Some limitations should be acknowledged. First, the sample size was relatively small, which may have resulted in low statistical power to detect gene expression differences between polyp samples and control samples. Thus, our results were of a preliminary nature. Despite this disadvantage, the present study was powered to identify DEGs that exhibited large fold changes with high statistical significance. Moreover, there were some consistency between our findings and the previous studies [6,7,13,21,35]. Hence, the results of our analysis could be reliable to a large extent. Second, our findings were obtained based on the bioinformatics methods and computational analysis. There was a lack of experimental validation for these findings in the present study. Therefore, further investigation, by means of RT-PCR, Western blotting, and immunohistochemistry, is needed to verify our results.

5. Conclusions

In summary, using multiple bioinformatics tools, we conducted a comprehensive analysis of gene expression profiles to identify several key genes and signaling pathways associated with the pathogenesis of CRSwNP. The results of the present study may provide new perspectives on the development of effective therapeutic strategies for patients with CRSwNP. However, further experimentation and additional studies with large sample sizes are required to confirm these findings.

Compliance with ethical standards

Declarations of interest

None.

Funding

This research did not receive any specific grant from funding agencies in the public, commercial, or not-for-profit sectors.

References

[1] Orlandi RR, Kingdom TT, Hwang PH, Smith TL, Alt JA, Baroody FM, et al. International consensus statement on allergy and rhinology: rhinosinusitis. Int Forum Allergy Rhinol 2016;6(Suppl. 1):S22–209. https://doi.org/10.1002/alr.21695.

[2] Fokkens WJ, Lund VJ, Mullol J, Bachert C, Alobid I, Baroody F, et al. EPOS 2012: European position paper on rhinosinusitis and nasal polyps 2012. A summary for otorhinolaryngologists. Rhinology 2012;50:1–12. https://doi.org/10.4193/Rhino50E2.

[3] Stevens WW, Schleimer RP, Kern RC. Chronic rhinosinusitis with nasal polyps. J Allergy Clin Immunol Pract 2016;4:565–72. https://doi.org/10.1016/j.jaip.2016.04.012.

[4] Bachert C, Akdis CA. Phenotypes and emerging endotypes of chronic rhinosinusitis. J Allergy Clin Immunol Pract 2016;4:621–8. https://doi.org/10.1016/j.jaip.2016.05.004.

[5] Bachert C, Zhang L, Gevaert P. Current and future treatment options for adult chronic rhinosinusitis: focus on nasal polyposis. J Allergy Clin Immunol 2015;136:1431–40. https://doi.org/10.1016/j.jaci.2015.10.010.

[6] Plager DA, Kahl JC, Asmann YW, Nilson AE, Pallanch JF, Friedman O, et al. Gene transcription changes in asthmatic chronic rhinosinusitis with nasal polyps and comparison to those in atopic dermatitis. PLoS One 2010;5:e11450https://doi.org/10.1371/journal.pone.0011450.

[7] Stankovic KM, Goldsztein H, Reh DD, Platt MP, Metson R. Gene expression profiling of nasal polyps associated with chronic sinusitis and aspirin-sensitive asthma. Laryngoscope 2008;118:881–9. https://doi.org/10.1097/MLG.0b013e31816b4b6f.

[8] Liu Z, Kim J, Sypek JP, Wang IM, Horton H, Oppenheim FG, et al. Gene expression profiles in human nasal polyp tissues studied by means of DNA microarray. J Allergy Clin Immunol 2004;114:783–90. https://doi.org/10.1016/j.jaci.2004.04.052.

[9] Barrett T, Wilhite SE, Ledoux P, Evangelista C, Kim IF, Tomashevsky M, et al. NCBI GEO: archive for functional genomics data sets—update. Nucleic Acids Res 2013;41:D991–5. https://doi.org/10.1093/nar/gks1193.

[10] Kolesnikov N, Hastings E, Keays M, Melnichuk O, Tang YA, Williams E, et al.

ArrayExpress update—simplifying data submissions. Nucleic Acids Res 2015;43:D1113–6. https://doi.org/10.1093/nar/gku1057.

[11] Rouillard AD, Wang Z, Ma'ayan A. Reprint of “Abstraction for data integration: fusing mammalian molecular, cellular and phenotype big datasets for better knowledge extraction”. Comput Biol Chem 2015;59(Pt B):123–38. https://doi.org/10.1016/j.compbiolchem.2015.08.005.

[12] Jones AC, Bosco A. Using network analysis to understand severe asthma phenotypes. Am J Respir Crit Care Med 2017;195:1409–11. https://doi.org/10.1164/rccm.201612-2572ED.

[13] Seshadri S, Lin DC, Rosati M, Carter RG, Norton JE, Suh L, et al. Reduced expression of antimicrobial PLUNC proteins in nasal polyp tissues of patients with chronic rhinosinusitis. Allergy 2012;67:920–8. https://doi.org/10.1111/j.1398-9995.2012.02848.x.

[14] Meltzer EO, Hamilos DL, Hadley JA, Lanza DC, Marple BF, Nicklas RA, et al. Rhinosinusitis: establishing definitions for clinical research and patient care. J Allergy Clin Immunol 2004;114:155–212. https://doi.org/10.1016/j.jaci.2004.09.029.

[15] Gautier L, Cope L, Bolstad BM, Irizarry RA. affy—analysis of Affymetrix GeneChip data at the probe level. Bioinformatics 2004;20:307–15. https://doi.org/10.1093/bioinformatics/btg405.

[16] Ritchie ME, Phipson B, Wu D, Hu Y, Law CW, Shi W, et al. limma powers differential expression analyses for RNA-sequencing and microarray studies. Nucleic Acids Res 2015;43:e47. https://doi.org/10.1093/nar/gkv007.

[17] Yu G, Wang LG, Han Y, He QY. clusterProfiler: an R package for comparing biological themes among gene clusters. OMICS 2012;16:284–7. https://doi.org/10.1089/omi.2011.0118.

[18] Szklarczyk D, Franceschini A, Wyder S, Forslund K, Heller D, Huerta-Cepas J, et al. STRING v10: protein-protein interaction networks, integrated over the tree of life. Nucleic Acids Res 2015;43:D447–52. https://doi.org/10.1093/nar/gku1003.

[19] Bader GD, Hogue CW. An automated method for finding molecular complexes in large protein interaction networks. BMC Bioinf 2003;4(2). https://doi.org/10.1186/1471-2105-4-2.

[20] Li CW, Zhang KK, Li TY, Lin ZB, Li YY, Curotto de Lafaille MA, et al. Expression profiles of regulatory and helper T-cell-associated genes in nasal polyposis. Allergy 2012;67:732–40. https://doi.org/10.1111/j.1398-9995.2012.02811.x.

[21] Peterson S, Poposki JA, Nagarkar DR, Chustz RT, Peters AT, Suh LA, et al. Increased expression of CC chemokine ligand 18 in patients with chronic rhinosinusitis with nasal polyps. J Allergy Clin Immunol 2012;129:119–27. https://doi.org/10.1016/j.jaci.2011.08.021.

[22] Legrand F, Tomasevic N, Simakova O, Lee CC, Wang Z, Raffeld M, et al. The eosinophil surface receptor epidermal growth factor-like module containing mucin-like hormone receptor 1 (EMR1): a novel therapeutic target for eosinophilic disorders. J Allergy Clin Immunol 2014;133:1439–47. https://doi.org/10.1016/j.jaci.2013.11.041.

[23] Beeley JA. Basic proline-rich proteins: multifunctional defence molecules? Oral Dis 2001;7:69–70. https://doi.org/10.1034/j.1601-0825.2001.70201.x.

[24] Bingle CD, Craven CJ. PLUNC: a novel family of candidate host defence proteins expressed in the upper airways and nasopharynx. Hum Mol Genet 2002;11:937–43. https://doi.org/10.1093/hmg/11.8.937.

[25] Wijkstrom-Frei C, El-Chemaly S, Ali-Rachedi R, Gerson C, Cobas MA, Forteza R, et al. Lactoperoxidase and human airway host defense. Am J Respir Cell Mol Biol 2003;29:206–12. https://doi.org/10.1165/rcmb.2002-0152OC.

[26] Yin A, Margolis HC, Grogan J, Yao Y, Troxler RF, Oppenheim FG. Physical parameters of hydroxyapatite adsorption and effect on candidacidal activity of histatins. Arch Oral Biol 2003;48:361–8. https://doi.org/10.1016/S0003-9969(03)00012-8.

[27] Sadrzadeh SM, Bozorgmehr J. Haptoglobin phenotypes in health and disorders. Am J Clin Pathol 2004;121(Suppl):S97–104. https://doi.org/10.1309/8glx5798y5xhq0vw.

[28] Brescia G, Zanotti C, Parrino D, Barion U, Marioni G. Nasal polyposis pathophysiology: endotype and phenotype open issues. Am J Otolaryngol 2018;39:441–4. https://doi.org/10.1016/j.amjoto.2018.03.020.

[29] Kato A. Immunopathology of chronic rhinosinusitis. Allergol Int 2015;64:121–30. https://doi.org/10.1016/j.alit.2014.12.006.

[30] Paradowska-Gorycka A, Jurkowska M. Structure, expression pattern and biological activity of molecular complex TREM-2/DAP12. Hum Immunol 2013;74:730–7. https://doi.org/10.1016/j.humimm.2013.02.003.

[31] Tessarz AS, Cerwenka A. The TREM-1/DAP12 pathway. Immunol Lett 2008;116:111–6. https://doi.org/10.1016/j.imlet.2007.11.021.

[32] Turnbull IR, Colonna M. Activating and inhibitory functions of DAP12. Nat Rev Immunol 2007;7:155–61. https://doi.org/10.1038/nri2014.

[33] Takaki R, Watson SR, Lanier LL. DAP12: an adapter protein with dual functionality. Immunol Rev 2006;214:118–29. https://doi.org/10.1111/j.1600-065X.2006.00466.x.

[34] Peng Q, Malhotra S, Torchia JA, Kerr WG, Coggeshall KM, Humphrey MB. TREM2- and DAP12-dependent activation of PI3K requires DAP10 and is inhibited by SHIP1. Sci Signal 2010;3:ra38. https://doi.org/10.1126/scisignal.2000500.

[35] Lee JY, Lee SH, Lee HM, Lee SH, Jung HH, Lee SW, et al. Analysis of gene expression profiles of normal human nasal mucosa and nasal polyp tissues by SAGE. J Allergy Clin Immunol 2006;118:134–42. https://doi.org/10.1016/j.jaci.2006.02.048.

[36] Schwindinger WF, Robishaw JD. Heterotrimeric G-protein betagamma-dimers in growth and differentiation. Oncogene 2001;20:1653–60. https://doi.org/10.1038/sj.onc.1204181.

[37] Leung T, Chen H, Stauffer AM, Giger KE, Sinha S, Horstick EJ, et al. Zebrafish G protein gamma2 is required for VEGF signaling during angiogenesis. Blood 2006;108:160–6. https://doi.org/10.1182/blood-2005-09-3706.

[38] Bobic S, Hox V, Callebaut I, Vinckier S, Jonckx B, Stassen JM, et al. Vascular endothelial growth factor receptor 1 expression in nasal polyp tissue. Allergy 2014;69:237–45. https://doi.org/10.1111/all.12277.

[39] Ono SJ, Nakamura T, Miyazaki D, Ohbayashi M, Dawson M, Toda M. Chemokines: roles in leukocyte development, trafficking, and effector function. J Allergy Clin Immunol 2003;111:1185–99. https://doi.org/10.1067/mai.2003.1594.